

# Supporting Information: Dynamic Imine Bonding Facilitates Mannan Release from a Nanofibrous Peptide Hydrogel

Brett H. Pogostin,<sup>†</sup> Gabriel Saenz,<sup>‡</sup> Carson C. Cole,<sup>‡</sup> Erin M. Euliano,<sup>†</sup> Jeffrey D. Hartgerink,<sup>\*</sup>  
<sup>†,‡</sup> and Kevin J. McHugh<sup>\*</sup>, <sup>†,‡</sup>

<sup>\*</sup> Corresponding Authors

Email: [jdh@rice.edu](mailto:jdh@rice.edu); [kevin.mchugh@rice.edu](mailto:kevin.mchugh@rice.edu)

Tel: +1 (713) 348-2101; +1 (713) 348-8089

<sup>†</sup> Department of Bioengineering, Rice University, Houston, TX, 77005, USA

<sup>‡</sup> Department of Chemistry, Rice University, Houston, TX, 77005, USA

## Contents:

Figure S1: SEC of Man and R-Man	SI-2
Figure S2: FTIR of E <sub>2</sub> Loaded with O-Man and R-Man	SI-2
Figure S3: Negative Stain TEM of R-Man	SI-3
Figure S4: K <sub>2</sub> Hydrogel Frequency Sweeps	SI-3
Figure S5: E <sub>2</sub> Rheology	SI-4
Figure S6: Custom 3D-Printed Release Plate	SI-4
Figure S7: <i>In vitro</i> Release from E <sub>2</sub>	SI-5
Figure S8: Full <i>In Vivo</i> Release Data	SI-5
Figure S9: Gly + O-Man <i>In Vivo</i> Release Data	SI-6
Figure S10: MALDI and UPLC of K <sub>2</sub> Peptide	SI-6
Figure S11: MALDI and UPLC of E <sub>2</sub> Peptide	SI-7

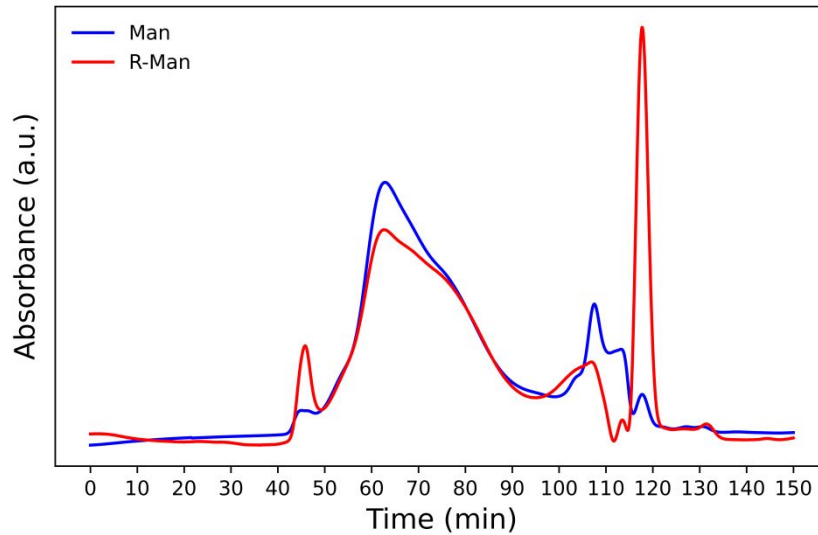


**Figure S1.** Size exclusion chromatography of unmodified mannan (Man; blue) and reduced mannan (R-Man; red) shows that the majority of the carbohydrate remains unchanged after synthesis. The large molecular weight distribution of mannan is expected as the carbohydrate from the supplier ranges from 60 kDa to 30 kDa. The peak at 120 min in the R-Man sample suggests that some chain shortening may occur from oxidation; however, this low molecular weight peak makes up less than 15% of the total area under the curve. The chromatograms were area normalized and absorbance is shown in arbitrary units.

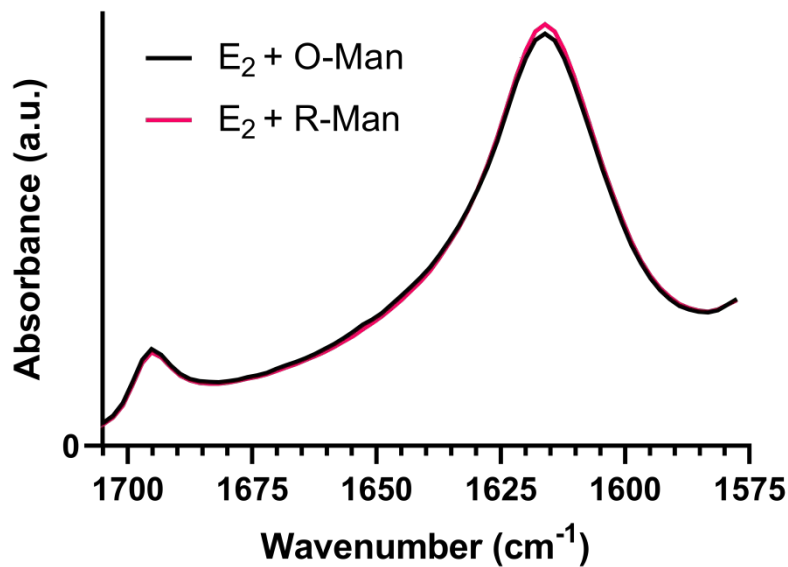


**Figure S2.** FTIR spectra of  $E_2$  loaded with O-Man and R-Man are nearly identical, suggesting that there are no differences in secondary structure and no imine bonding occurring between the oxidized carbohydrate and the  $E_2$  peptide.

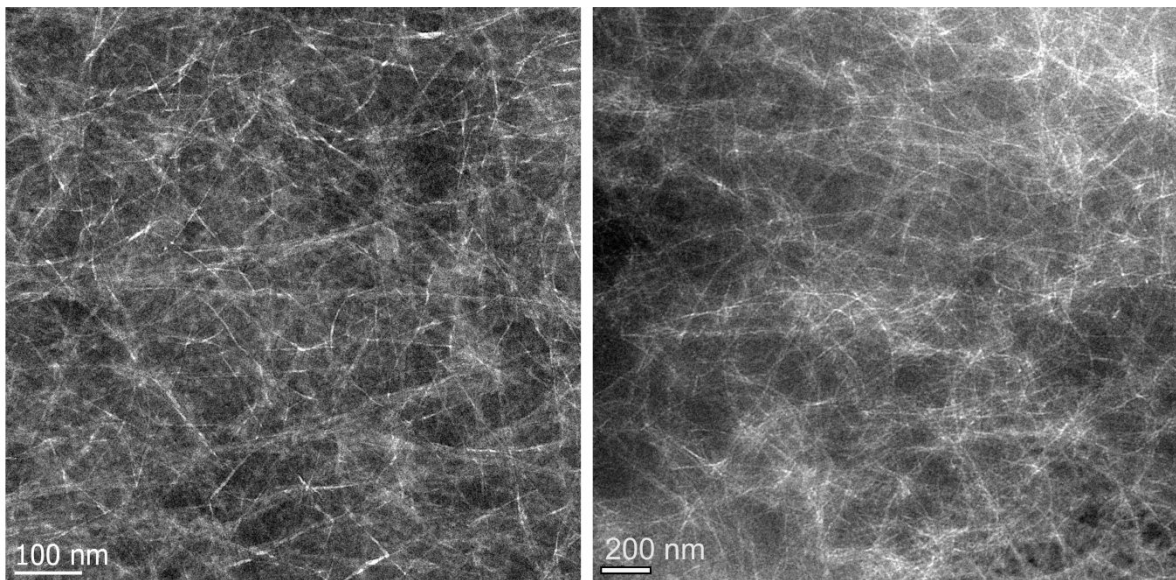


**Figure S3.** Negative stain TEM micrographs of R-Man show different morphologies depending on the location on the sample the image is taken. These differences are likely an artifact of drying necessary for sample preparation.

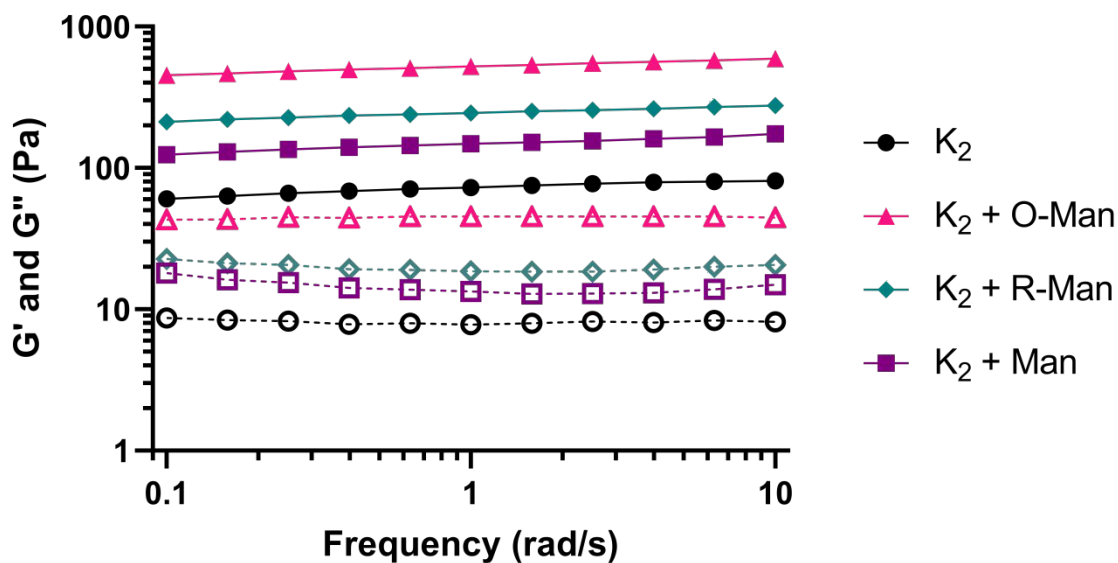


**Figure S4.** Frequency sweeps from 0.1-10 rad/s on a representative sample of K<sub>2</sub>, K<sub>2</sub> loaded with O-Man (K<sub>2</sub> + O-Man), K<sub>2</sub> loaded with Red-Man (K<sub>2</sub> + Red-Man), and K<sub>2</sub> loaded with unmodified Man (K<sub>2</sub> + Man). Filled symbols represent  $G'$  and empty symbols represent  $G''$  values. All materials showed hydrogel character as indicated by  $G' > G''$ . The values of  $G'$  and  $G''$  were largely linear over the frequency regime tested.

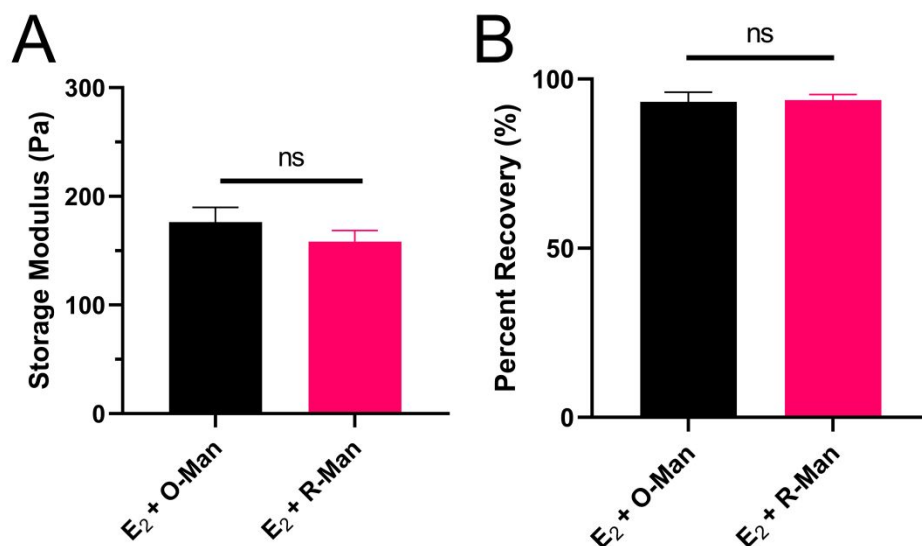


**Figure S5.** Rheological characterization of E<sub>2</sub> loaded with O-Man and R-Man. A) The storage moduli of O-Man loaded E<sub>2</sub> and R-Man loaded E<sub>2</sub> are  $176 \pm 11$  Pa and  $158 \pm 8$  Pa, respectively. B) The percent recovery of the storage modulus 10 min after a 200% strain of O-Man loaded E<sub>2</sub> and R-Man loaded E<sub>2</sub> are  $93\% \pm 2\%$  and  $93\% \pm 1\%$ , respectively. There were no statistically significant differences in the rheological properties of the two samples.

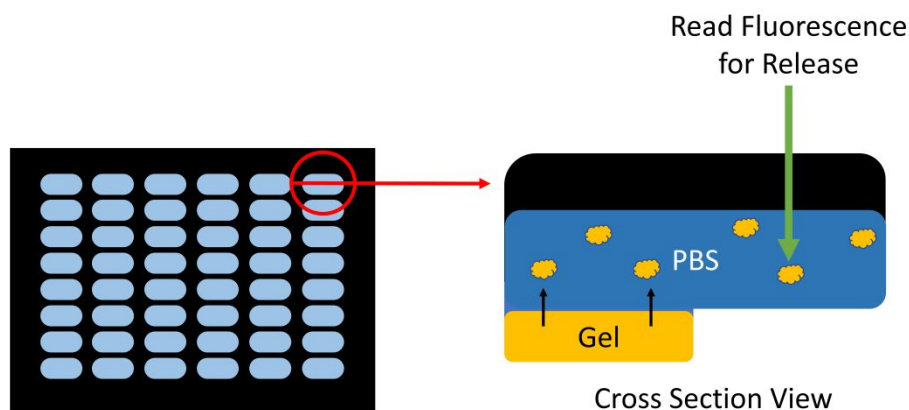


**Figure S6.** Schematic showing *in vitro* equilibrium release assay setup with custom 3D-printed 48-well plate. The plate was constructed by converting two adjacent wells of a 96-well plate into one oblong well (left sub-figure). As the cross section shows (right sub-figure), on the left half of the well there is a depression where the hydrogel is loaded. PBS is added on top and the loaded fluorescent payload releases into the supernatant. The fluorescent intensity of the supernatant is read on the right side of the well as the hydrogel so that only the fluorescence of the material in solution is measured.

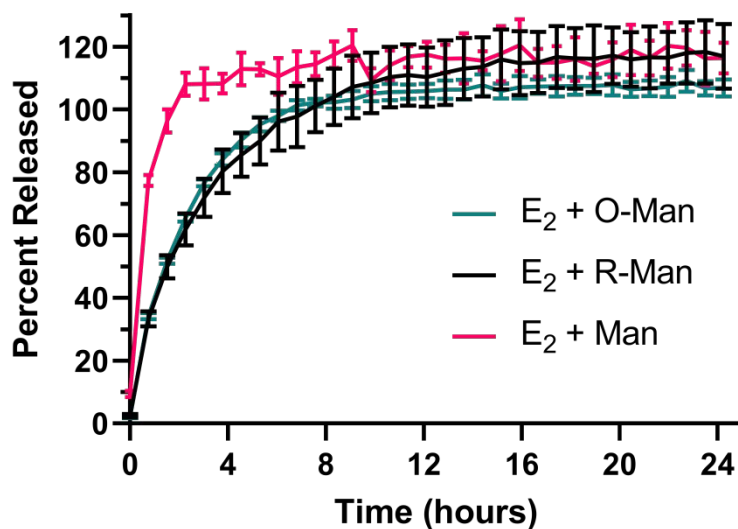


**Figure S7.** *In vitro* release results of E<sub>2</sub> loaded with oxidized mannan (E<sub>2</sub> + O-Man), reduced mannan (E<sub>2</sub> + R-Man), and unmodified mannan (E<sub>2</sub> + Man). The results show that Man releases the fastest from the negatively charged E<sub>2</sub>. O-Man and R-Man have similar release curves, suggesting that the delay in release from K<sub>2</sub> is due to imine bonding. Since this release assay is an equilibrium assay without media replacement, release values over 100% are indicative of repulsive interactions between the peptide and the carbohydrate enriching the amount of carbohydrate in the supernatant. This might be due to negative charges on the mannan of the carbohydrate or some other interaction that is not present in K<sub>2</sub>.

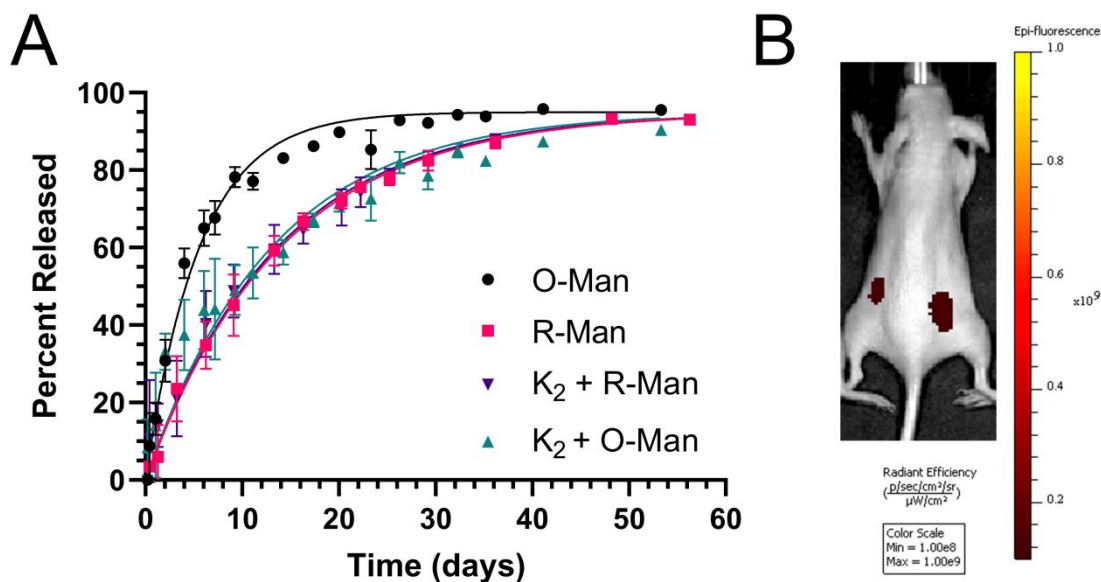


**Figure S8.** (A) Full 60-day *in vivo* release data fit with first-order release models for each group as described in the experimental procedures section. (B) IVIS image showing residual fluorescence in a representative mouse bilaterally injected with O-Man only at the end of the study showing that approximately 5% of the material remains at the injection site by the end of the monitoring period.

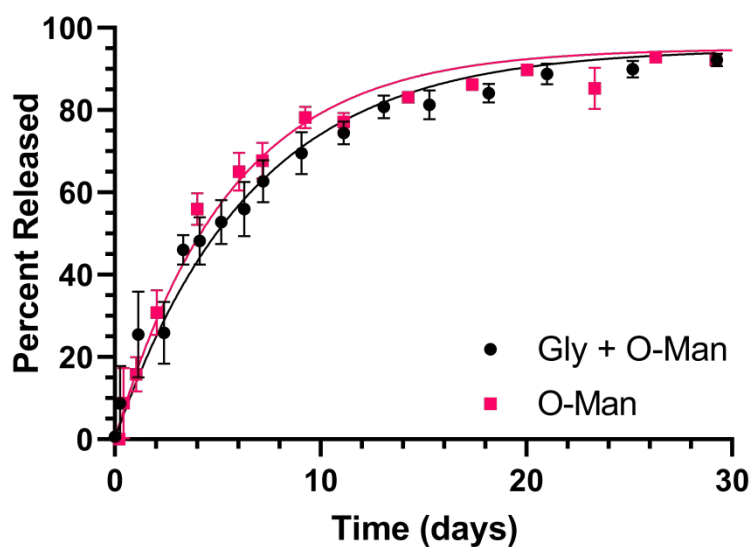


**Figure S9.** Release rates of O-Man alone and O-Man pretreated with excess glycine to quench reactive aldehyde groups. No significant difference in release rates was observed between the two groups over a 30-day period.

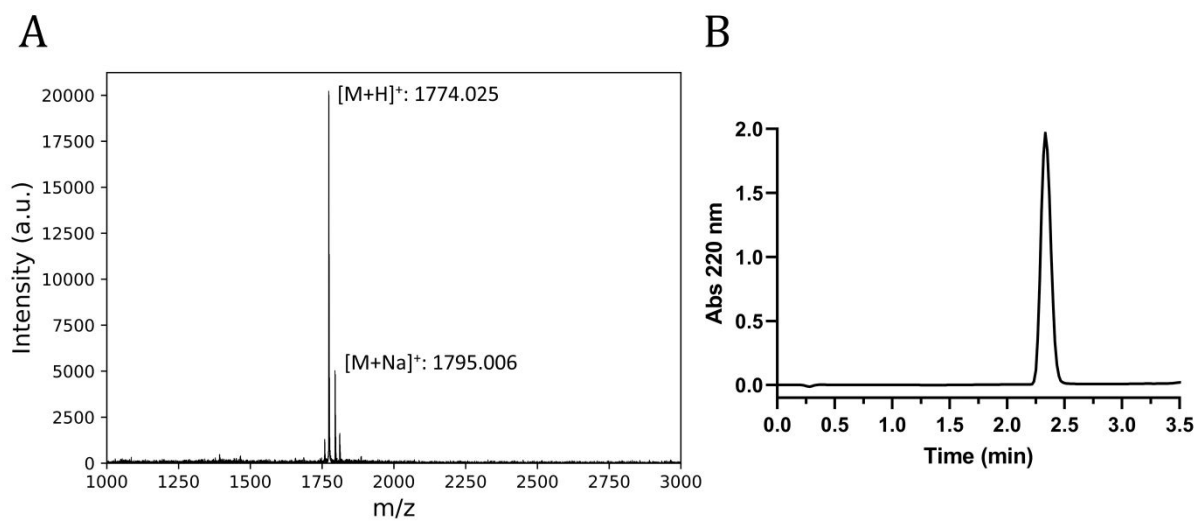


**Figure S10.** A) MALDI MS of HPLC-purified  $K_2$  observed  $[M+H]^+$ : 1774.025, expected  $[M+H]^+$ : 1774.29. B) UPLC trace of peptide. The presence of a single peak confirms purity.

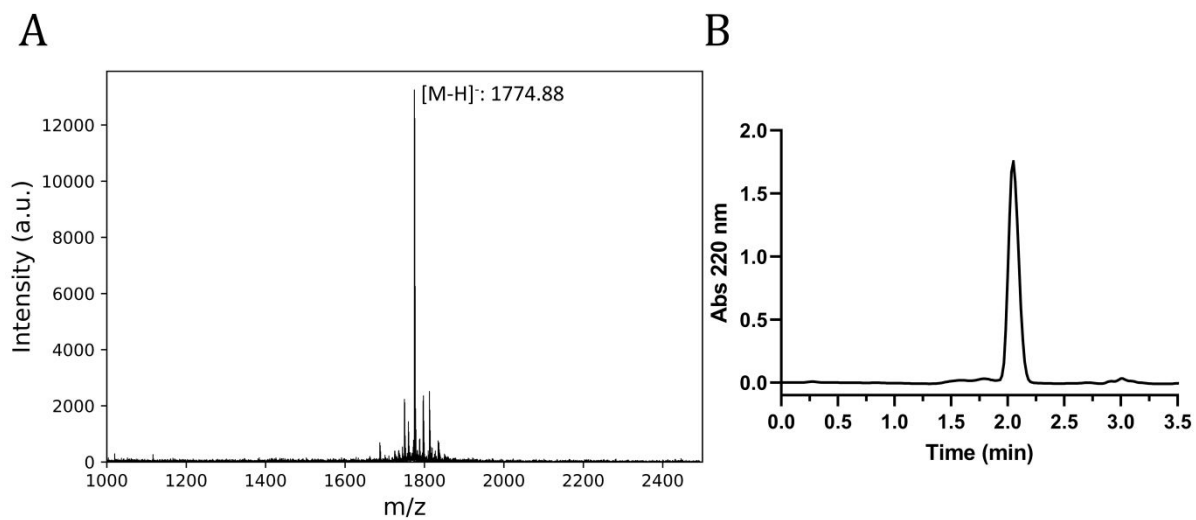


**Figure S11.** A) MALDI MS of HPLC-purified E<sub>2</sub> observed [M-H]: 1774.88, expected [M-H]: 1774.90. B) UPLC trace of peptide. The presence of a single peak confirms purity.